

# Micro-Bubble Phenomenon in Nanoscale Water-based Lubricating Film Induced by External Electric Field

Guoxin Xie · Jianbin Luo · Shuhai Liu ·  
Chenhui Zhang · Xinchun Lu

Received: 2 November 2007 / Accepted: 3 December 2007 / Published online: 26 January 2008  
© Springer Science+Business Media, LLC 2008

**Abstract** The effect of an external electric field (EEF) on water-based thin films has been investigated. Some micro-bubbles emerging around the edge of the Hertz contact region in the films of deionized water and polyethylene glycols (PEG) aqueous solutions have been observed. A higher EEF intensity is needed at which the micro-bubbles begin to emerge after the EEF is applied on the liquid film, which is defined as the threshold EEF intensity. The threshold EEF intensity increases with the molecular weight of PEG solution at lower molecular weight. There is a maximum value when the molecular weight reaches 10,000 Da, beyond which the threshold EEF intensity tends to decrease. The threshold EEF intensity also increases with the concentration of PEG solution. Micro-bubble emerging at negative EEF is easier than at positive EEF. The micro-bubble emerging in the film of deionized water is sensitive to the variation of EEF intensity, and disappears eventually as time progresses.

**Keywords** Gas micro-bubble · Cavitation ·  
Water-based lubrication · External electric field

## 1 Introduction

Water-based lubricants such as emulsions [1] are widely used in many fields such as metal working, journal bearing lubrication, and hydraulics since they combine excellent cooling efficiency and good lubricating properties.

Advanced ceramics, e.g.,  $\text{Al}_2\text{O}_3$  and  $\text{Si}_3\text{N}_4$  [2, 3], started to be considered as promising materials for sliding bearings and mechanical seals working in water due to its excellent tribological properties such as anti-wear, anti-seizure, anti-corrosion while it slides against the same material in water [4]. However, water itself has some disadvantages, such as high freezing point, oxidization, low viscosity, and very low pressure-viscosity, which hinder its use as a lubricant. Part of these disadvantages can be recovered by adding some water-soluble polymers, such as polyethylene glycols (PEG), which could enhance the viscosity index and electrical conductance [5, 6], etc. Moreover, cavitation, which is a phenomenon that sequential formation, growth and collapse of millions of micro-bubbles (voids) exist in liquid and consequently have the potential to result in the loss of material on the solid surface, is also a serious problem in water lubricants. Ventilation from ambient atmosphere, dissolved gas, and the vapor pressure in a liquid exceeds the ambient are considered to be the main reasons for the origin of micro-bubbles in the liquid resulting in cavitation [7, 8].

It has been revealed that shaft potentials frequently exist in rotating machinery such as turbines and compressors as a result of asymmetries of various faults, i.e., winding faults, unbalanced supplies, electrostatic effects, magnetized shaft, asymmetries of magnetic fields, etc. [9, 10]. In this case, the effect of an external electric field (EEF) on lubrication [11, 12] and wear [13, 14] properties evoked much interest among researchers. It has also been reported that micro-bubbles can be formed in dielectric liquids when sufficient high electric field is applied [15]. With miniaturization and reduction in the mass and inertial properties of components in machines, the loads applied to the mating members in contact have been dramatically reduced in recent years. This trend has resulted in the formation of vanishing narrow conjunctions, with an ultra-thin lubricant

G. Xie · J. Luo (✉) · S. Liu · C. Zhang · X. Lu  
State Key Laboratory of Tribology, Tsinghua University,  
Beijing 100084, P.R. China  
e-mail: luojb@tsinghua.edu.cn

G. Xie  
e-mail: xie-gx@163.com

film of the order of a few to tens of nanometers [16], thus a small potential drop could readily induce micro-bubble emerging in the nanoscale thin liquid film [17]. In the present article, the effect of EEF on micro-bubble emerging phenomenon in water-based film including deionized water and polyethylene glycols (PEG) aqueous solutions is investigated using the method of relative optical interference intensity (ROII), thereby providing some valuable guidances to the cavitation prevention in water-based journal bearings.

## 2 Experimental

The experimental setup is shown in Fig. 1. A liquid film is formed between a surface of a glass disk coated with a semi-reflective chromium (Cr) layer prepared by the high vacuum thermal evaporation method and a surface of a highly polished steel ball (E52100) with a diameter of 22.23 mm. A silica layer with a thickness of 300 nm has been coated on the surface of the Cr layer, and it is a film thickness measuring technique which is normally used in the ROII method [18, 19] and the spacer layer imaging method (SLIM) [20]. Monochromatic light is shone through the glass disk into the contact, and when the beam of the light reaches the upper surface of the Cr layer, it is split into two beams—one is reflected at the upper surface of the Cr layer and the other passes through the Cr layer and the lubricant film, and is then reflected at the surface of the steel ball. Since the two beams come from the same light

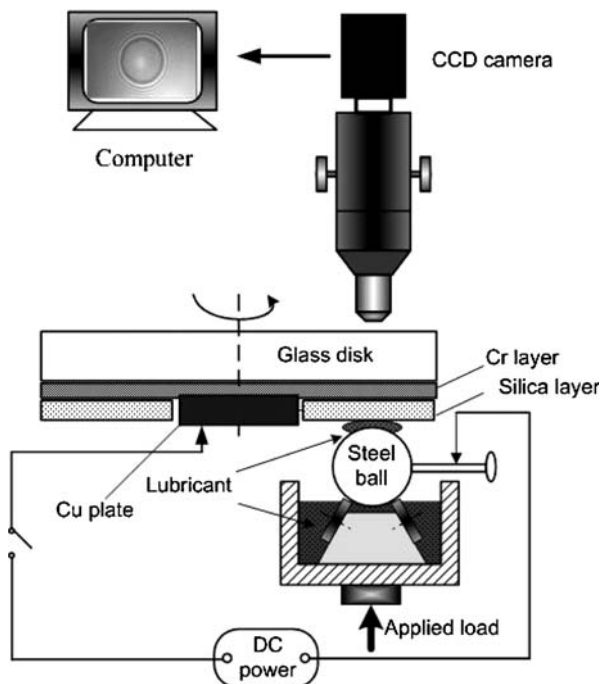


**Fig. 1** Schematic presentation of the test apparatus

source and have different optical paths, they will interfere with each other and the film thickness in the central region can be obtained from the optical interference intensity [18]. The appearance of liquid film in the computer is exhibited by the interference pattern with a CCD camera. The film thickness of static liquid film is calibrated by the air film, i.e., dry contact, the thickness of which is considered as zero. If the oil refractive index is 1.47 and the wavelength is 600 nm, the resolution of measured film thickness is smaller than 0.5 nm when the film thickness ranges from 5 to 55 nm. In addition, the resolution in the horizontal direction is 1.0 mm. For applying an external potential to the oil film, one end of the direct current (DC) power keeps contacting with the Cr layer through a copper plate, and the other end contacts a shaft welded on the steel ball through an electric brush. A static contact was adopted in order to avoid the multifactor across impact in dynamic process. The applied load is 4 N, which corresponds to the average Hertz pressure of 117 MPa.

During the experiments, deionized water and PEG aqueous solutions with different molecular weights from 600 to 20,000 Da and different concentrations from 0 to 30% were used as tested liquids. Their viscosity, contact angle, dielectric constant, and electrical conductance are listed in Table 1. Surface tension measurement was conducted using KrUss K12 Tensiometer. A controlled-strain-rate Hake RV20 rheometer with concentric cylinder geometry was used to measure the viscosity, and the shear rate adopted was  $500 \text{ s}^{-1}$ . An HK-307 type electric conductivity meter was employed to measure the electric conductivity of all liquids. A PNA series microwave network analyzers provided by Agilent Corporation was used to measure the dielectric constant, and the frequency range adopted was from 100 Hz to 40 MHz. In this study, the EEF polarity was also changed to investigate its effect on the liquid film, and positive potential means that the steel ball is at a higher potential than glass disk and vice versa for negative potential. The experiment was performed at a temperature of  $25 \pm 1 \text{ }^\circ\text{C}$ .

## 3 Results and Discussion

### 3.1 The Effect of Molecular Weight of PEG on Micro-Bubble Emerging

The relationship between molecular weight and threshold EEF intensity for micro-bubble emerging is shown in Fig. 2. The EEF intensity in the present article denotes the one applied to the liquid film itself, excluding the silica layer, which could be expressed as follows [21]:

$$E = U \varepsilon_{\text{silica}} (h_0 \varepsilon_{\text{silica}} + h_{\text{silica}} \varepsilon_{\text{liquid}})^{-1}, \quad (1)$$

**Table 1** Physical parameters of different PEG aqueous solutions

|  |        | Viscosity<br>(mPa s) | Electric<br>conductivity<br>( $10^{-4} \Omega^{-1} \text{m}^{-1}$ ) | Relative<br>permittivity | Surface<br>tension<br>(mN/m) |
|--|--------|----------------------|---|--------------------------|------------------------------|
| Molecular weight<br>(concentration<br>15%)       | 600    | 1.561                | 84.30   | 39.17                    | 77.78                        |
|  | 1,000  | 1.651                | 21.30   | 40.69                    | 82.80                        |
|  | 2,000  | 2.230                | 15.28   | 39.75                    | 78.57                        |
|  | 6,000  | 6.543                | 56.10   | 40.71                    | 81.30                        |
|  | 10,000 | 11.296               | 32.30   | 40.67                    | 87.89                        |
|  | 20,000 | 18.798               | 39.30   | 39.97                    | 86.94                        |
| Concentration<br>(molecular<br>weight PEG 1,000) | 0%     | 0.380                | 3.24  | 78.69                    | 72.84                        |
|  | 1%     | 0.514                | 4.91  | 44.19                    | 90.13                        |
|  | 5%     | 0.819                | 15.34   | 43.28                    | 89.39                        |
|  | 10%    | 1.414                | 19.02   | 42.26                    | 90.59                        |
|  | 15%    | 1.651                | 21.30   | 40.69                    | 82.80                        |
|  | 30%    | 5.487                | 15.90   | 35.05                    | 88.80                        |

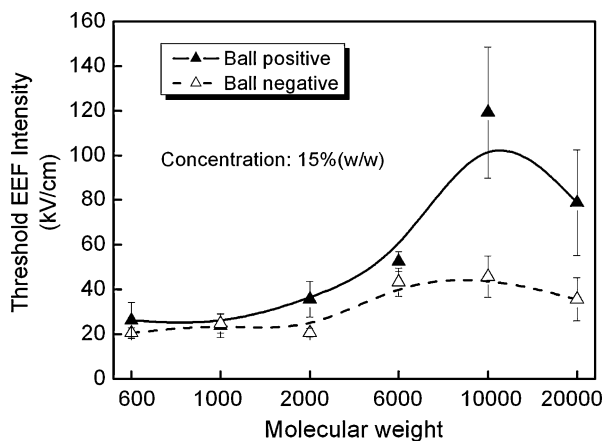


**Fig. 2** Effect of molecular weight on the threshold EEF intensity for micro-bubble emergence. The solid triangular symbols represent positive potential applied, and the hollow ones represent negative potential. All the tested PEG aqueous solutions are with the concentration of 15% (w/w)

where,  $E$  is the electric field strength inside the contact zone;  $U$  is the total potential applied to the whole circuit;  $\epsilon_{\text{liquid}}$  and  $\epsilon_{\text{silica}}$  are the relative permittivity of the liquid film and silica film, respectively, and  $h_0$  is the static liquid film thickness in the contact region, which is in the range from 8 to 15 nm for different liquid films.  $h_{\text{silica}}$  is the thickness of silica film. It can be seen from Fig. 2 that when molecular weight is relatively lower, such as PEG 600 and PEG 1,000, the EEF intensity for micro-bubble emerging is very close to each other for positive and negative potentials. The threshold EEF intensity gradually elevates with molecular weight increasing to 10,000 Da, where relatively higher values occur (120 kV/cm for positive case and 40 kV/cm for negative case). However, when the molecular weight increases further to PEG 20,000, the EEF intensity value drops a little by a

percentage of approximately 30%. The interference patterns of the films of PEG solutions as shown in Fig. 3 indicate the influence of molecular weight on the micro-bubble phenomenon under an EEF intensity of 150 kV/cm. At lower molecular weight, as shown in Fig. 3a–c, the micro-bubbles emerging from the edge of the contact region are plentiful and intensive. In contrast, when the molecular weight reaches 6,000 Da, the number of micro-bubbles decreases greatly, while the micro-bubble size does not change too much (Fig. 3d). The micro-bubble of PEG 10,000 cannot be observed from the pattern in Fig. 3e at such EEF intensity as 150 kV/cm, and this can be verified by the fact that it has the highest threshold EEF intensity, as mentioned above. Compared with PEG 10,000, the micro-bubbles emerging from the film of PEG 20,000 can be observed but are very sparse, just 4–5 micro-bubble moving trajectories in Fig. 3f. As to the effect of molecular weight on the physical parameters of different PEG aqueous solutions in Table 1, the variation of viscosity is much more regular than the other two, i.e., electric conductivity, relative permittivity. The surface tension is found to present an increase with molecular weight, which is roughly in agreement with the variation of threshold EEF intensity for micro-bubble emerging.

### 3.2 The Effect of Concentration of PEG Solution on Micro-Bubble Emerging

The effect of concentration on the threshold EEF intensity for micro-bubble emergence is shown in Fig. 4. Clearly, when there is no PEG solute (the deionized water itself), the threshold EEF intensity value is about 25 kV/cm (positive potential). With the concentration increasing from 2.5 to 30%, the threshold EEF intensity value increases gradually for both positive and negative potential cases. When the

**Fig. 3** Interference patterns of the films of PEG solutions with different molecular weights when the positive EEF intensity was 150 kV/cm. (a) PEG 600, (b) PEG 1,000, (c) PEG 2,000, (d) PEG 6,000, (e) PEG 10,000, and (f) PEG 20,000

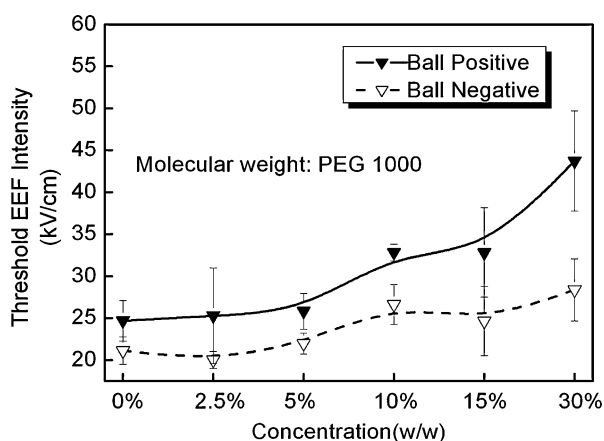
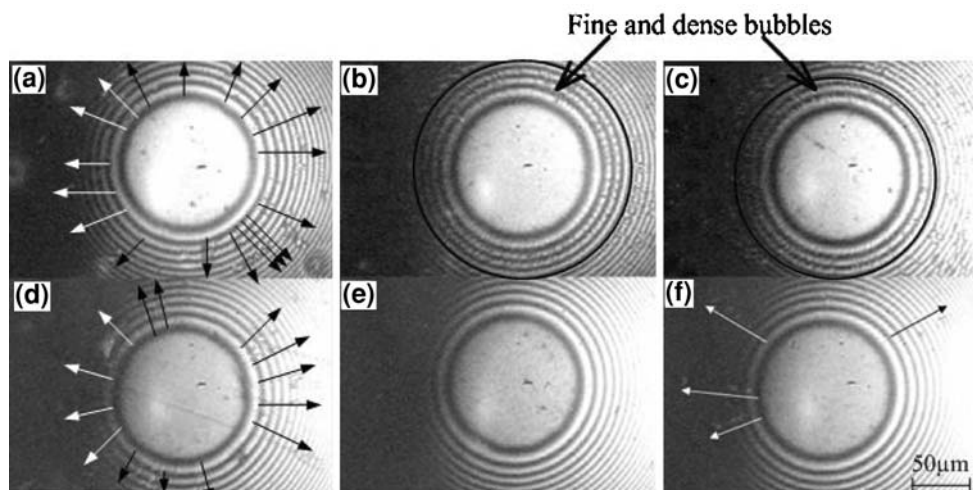


**Fig. 4** Effect of concentration of PEG solutions on the threshold EEF intensity for micro-bubble emergence. The solid triangular symbols represent positive potential applied, and the hollow ones represent negative potential. All the tested PEG aqueous solutions are with the molecular weight of 1,000 Da

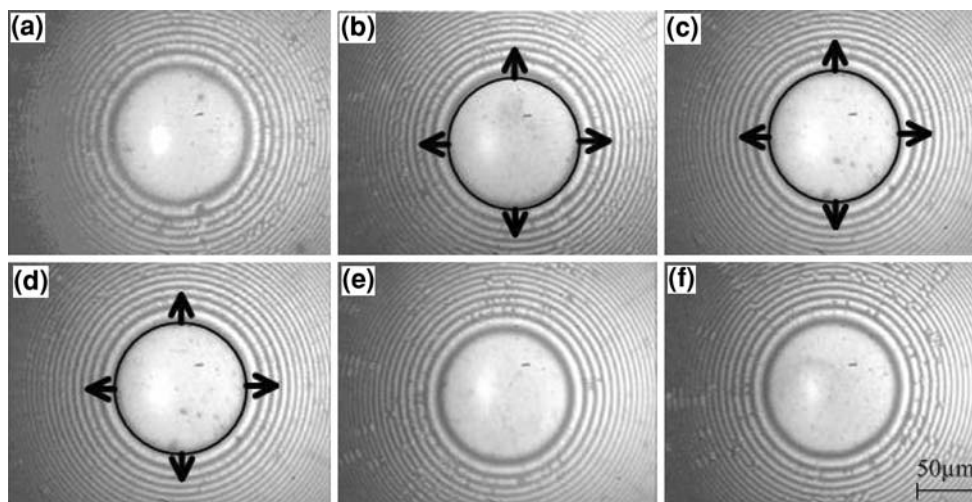
concentration equals to 30%, the threshold value reaches a relatively higher value (approximately 40 kV/cm). The interference patterns of the film PEG 1,000 aqueous solutions with different concentrations are shown in Fig. 5, where the EEF intensity was around 190 kV/cm. For the deionized water, the micro-bubble is so dense and small to be discriminated in the Fig. 5a, and many fine micro-bubbles' moving trajectories can be clearly observed from the video in the process of the experiment. When the concentration was increased to 2.5% (Fig. 4b) and 5% (Fig. 5c), the number of micro-bubbles' trajectories is still abundant, as indicated by the black circles and arrows. At concentration of 10%, the intensity of micro-bubbles seems to be weakened though the micro-bubbles can still be seen in Fig. 5d. However, the cases for higher concentrations are a little different from the former ones, e.g., the pattern of the film of PEG solution with concentration of 15% in Fig. 5e evidently shows the micro-bubbles go less but bigger, and

this trend is even more obvious when the concentration reaches 30%, as shown in Fig. 5f. In addition, it can be seen from Table 1 that the viscosity and electric conductivity increase with concentration, and relative permittivity has a decrease trend implying that adding more solute of PEG polymer can reduce the polarity of the solution. No obvious trend can be observed for the relationship between surface tension and concentration.

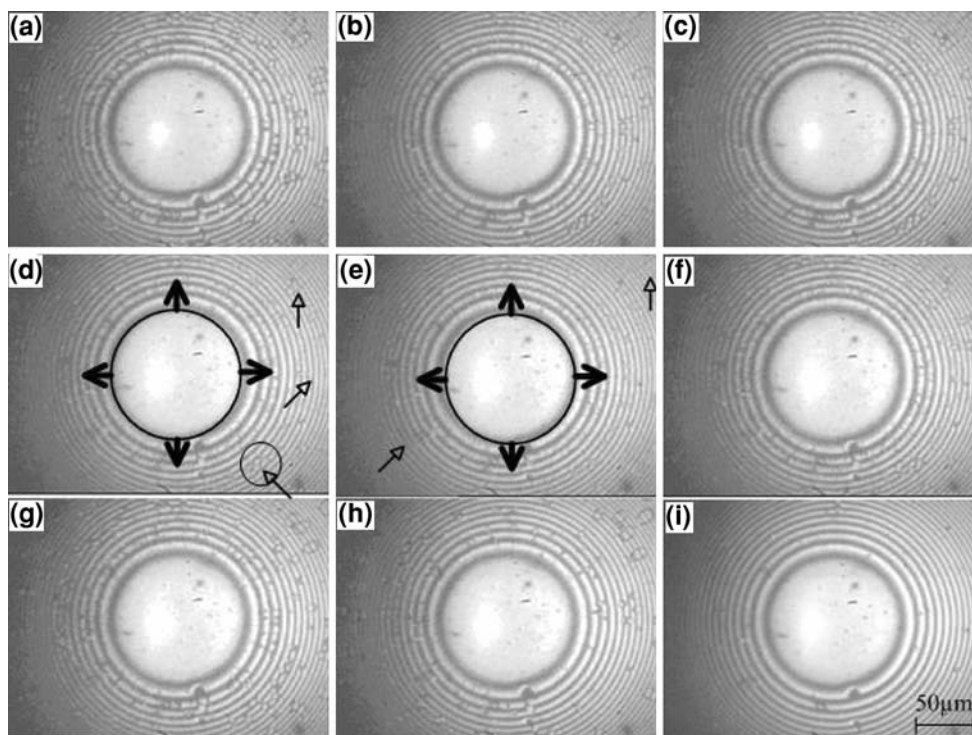
### 3.3 The Micro-Bubble Phenomenon in Deionized Water

Figure 6 shows the effect of EEF intensity on micro-bubble emerging in deionized water. As is shown above, the threshold EEF intensity of its micro-bubble emerging is around 25 kV/cm, so when applied with an EEF intensity of 30 kV/cm, abundant micro-bubbles moving away from the edge of contact region can be clearly observed in Fig. 6a, and their size is big enough to be distinguished in the graph not only near the contact region but far away from the contact region. When the field intensity was increased to 60 kV/cm (Fig. 6b) and 90 kV/cm (Fig. 6c), the micro-bubbles become so intensive and fine that they cannot be seen from the interference rings near the contact region, only some apparently bigger micro-bubbles can be distinctly discerned in the outer rings. When the EEF intensity was increased further, from 90 to 150 kV/cm, then up to 300 kV/cm, the static micro-bubbles in Fig. 6d, e cannot be captured anymore, and only quite fine and dense micro-bubble moving trajectories, like the streamlet, were observed with the aid of dynamic video during the experiment, and the phenomenon is indicated by black arrows. It should be pointed out that micro-bubble gathering phenomenon in the inner ring region does not appear here due to low viscosity of deionized water, and this is in contrast with glycerin [17]. From Fig. 6f on, the field intensity was gradually reduced,





**Fig. 5** Interference patterns of the films of PEG solutions with different concentrations when the positive EEF intensity was 190 kV/cm, (a) 0%, (b) 2.5%, (c) 5%, (d) 10%, (e) 15%, (f) 30%



**Fig. 6** The effect of EEF intensity on micro-bubble emerging in deionized water film under positive potential, (a) 30 kV/cm, (b) 60 kV/cm, (c) 90 kV/cm, (d) 150 kV/cm, (e) 300 kV/cm, (f) 150 kV/cm (back), (g) 60 kV/cm (back), (h) 30 kV/cm (back), (i) 0 kV/cm (back)

firstly to 150 kV/cm, then to 60 kV/cm (Fig. 6g) and 30 kV/cm (Fig. 6h), finally to 0 kV/cm (Fig. 6i), the micro-bubbles with relatively bigger size reoccur slowly, especially at the intensity of 60 kV/cm, the micro-bubbles with soybean shape become intensive and abundant again. Therefore, the micro-bubble emerging behavior in deionized water is sensitive to the variation of EEF intensity and relatively controllable.

Figure 7 gives different interference patterns of deionized water film at various times to illustrate the time effect of micro-bubble emerging for the case of positive potential. When it is 30 s at the initial period, the micro-bubbles moving away from the edge of contact region are obvious. The micro-bubbles are round shaped in the inner rings region though relatively smaller, and present bigger elliptical shape in the outer rings region. Then, the

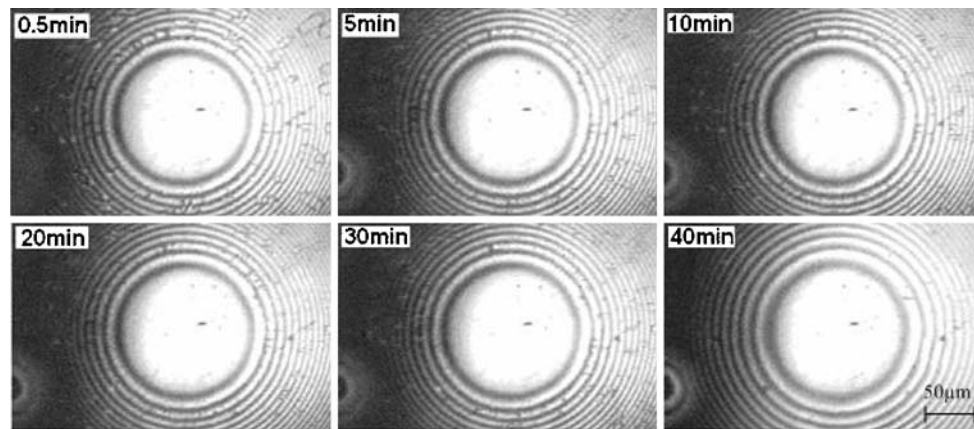


**Fig. 7** Snapshots of micro-bubble emerging in deionized water film at various times under a positive EEF intensity of 62.5 kV/cm

micro-bubbles become denser but smaller as time goes, e.g., at the time of 10 min, the smaller micro-bubbles are intensive and move faster so that the micro-bubbles far away from the contact region cannot be gathered to form larger elliptical micro-bubbles, which is different from the initial period. However, when the time increases further, the micro-bubbles seem to reduce a little, however, this reduction trend is not too apparent compared 30 min with 5 min. When the time reaches 40 min, the micro-bubbles eventually disappear, and the liquid film confined in between the gap is absent.

### 3.4 Discussion

The phenomenon of micro-bubble emerging around the central region has significant implication to the practical applications in water-based lubricating case, because a potential of only 2.5 V is necessary for micro-bubble to generate in water film with a thickness of 1  $\mu\text{m}$ . The emerging micro-bubbles can play an important role for originating bubble nucleation or directly collapse in high-pressure region. It is thought that EEF can stimulate supersaturated vapor condensation, decreasing the critical size of liquid drops and the work needed for their formation [22], and the contribution of local overheating due to electro-thermal effect, together with the vaporization in the liquid film induced by high EEF strength whenever a point of zero pressure develops in the liquid film and a vacuous cavity starts to form. A rough estimation of temperature rise in the contact region, which is simplified as a cylindrical heated volume, can be given as [23]

$$\Delta T = \frac{\sigma E^2 r^2}{2k} \quad (2)$$

where  $\sigma$  and  $k$  are the electric conductivity and thermal conductivity, respectively, and  $r$  is contact radius. At the threshold EEF intensity for micro-bubble emerging in

water film ( $\sigma = 3.24 \times 10^{-4} \Omega^{-1} \text{m}^{-1}$ ,  $k = 0.145 \text{Wk}^{-1} \text{m}^{-1}$ ) of 25 kV/cm, the temperature rise  $\Delta T$  is approximately 95  $^\circ\text{C}$ , showing a possibility to originate boiling and bubble nucleation. In addition, the minimum EEF intensity for development of a point of zero pressure can be written as [15]

$$E_m = 358 \sqrt{\frac{1}{\varepsilon} \left( P + \frac{2\delta}{R} \right)} \quad (3)$$

where  $\varepsilon$  is dielectric constant,  $\delta$  is the surface tension of the liquid, and  $P$  is the hydrostatic pressure, and can be substituted by the external applied pressure here for the thin thickness of the liquid film.  $R$  is the radius of the particle in the liquid, and can be viewed as a very small value, say 2 nm, since the thin liquid film with a thickness is of the order of several nanometers in this study. The effect of molecular weight and concentration on threshold EEF intensity for micro-bubble emergence can be due to the variation in surface tension, permittivity and viscosity between different liquids, and the EEF strengths required for the points of zero pressure to occur for the liquids in this study are shown in Fig. 8, and part of the parameters adopted is listed in Table 1. As can be seen, a similar trend to the experimental observation is confirmed, i.e., with the increase of molecular weight and concentration, the formation of zero pressure points becomes more difficult, thus making the micro-bubble emerging harder. Also, PEG, as a non-ionic surfactant, presents the hackle shape in the case without water, and the zigzag shape in the hydration state for the PEG molecules with lower molecular weight. However, when the molecular weight increases to a critical point, beyond which the PEG molecules tend to tangle, then the tangled molecules may in turn provide more chance for the formation of zero pressure points. In addition, breakdown was initiated by the bubble of vapor, and the breakdown strength increased with the increasing viscosity, which is consistent with the relationship between

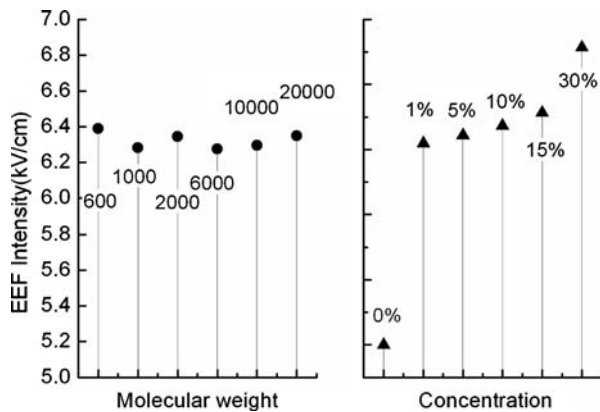


**Fig. 8** Calculated values for minimum EEF intensity required for zero pressure point to form for various liquid films of PEG aqueous solutions with different molecular weights and concentrations

threshold EEF intensity and viscosity in this study. Furthermore, the breakdown of liquid resulting in occurrence of electric current [24] can also accelerate the process of nucleation of micro-bubble due to the electro-thermal effect.

The difference of the threshold EEF intensity for micro-bubble emerging with different EEF polarities can be explained by electronic processes [25]. For the ball with negative potential case, the barrier to permit direct transfer of metal electrons of Fermi energy into the free electron states of the liquid is lowered by the EEF since the positive ions arriving at the steel ball build up a positive space charge stern layer adjacent to the ball to lower the barrier due to the oxide layer and perhaps organic layer. However, for the positive potential case, it can be safely assumed that such a silica film prepared by the high vacuum thermal evaporation will not be free of defects, at which an electron exchange may take place. So, the stern layer that exists near the silica layer can be weakened by the neutralization of positive ions from the liquid, thus the barrier for electron injection will not be lowered significantly, leading to the micro-bubble emerging harder compared with the negative case.

#### 4 Conclusion

Micro-bubbles in the films of PEG aqueous solutions and deionized water can be clearly observed. With the increase of molecular weight of PEG solution, the threshold EEF intensity for micro-bubble emerging increases, but there is a reverse trend when the molecular weight reaches 10,000 Da, and micro-bubbles in the film of PEG solutions with higher concentration are more difficult to generate due to the reduction of the polarity. The overheating effect plays a significant role in micro-bubble emerging. Micro-bubble can be easier to be induced when the steel ball was

applied with negative potential, and electronic process is used to account for it. The EEF intensity has great influence on the micro-bubbles' amount and intensity in water film, and as time progresses, the micro-bubbles gradually disappear.

**Acknowledgment** The work is financially supported by NSFC of China (50605034 and 50390062) by 973 Project (2007CB607604).

#### References

- Ratoi-Salagean, M., Spikes, H.A., Rieffe, H.L.: Optimizing film formation by oil-in-water emulsions. *Tribol. Trans.* **40**, 569–578 (1997)
- Wonga, H.C., Umehara, N., Kato, K.: The effect of surface roughness on friction of ceramics sliding in water. *Wear* **218**, 237–243 (1998)
- Wang, X.L., Kato, K., Adachi, K.: The lubrication effect of micro-pits on parallel sliding faces of SiC in water. *Tribol. Trans.* **45**, 294–301 (2002)
- Wong, H.C., Umehara, N., Kato, K.: Frictional characteristics of ceramics under water-lubricated conditions. *Tribol. Lett.* **5**, 303–308 (1998)
- Cai, J.L., Bo, S.Q., Cheng, R.S., Jiang, L.S., Yang, Y.: Analysis of interfacial phenomena of aqueous solutions of polyethylene oxide and polyethylene glycol flowing in hydrophilic and hydrophobic capillary viscometers. *J. Colloid Interface Sci.* **276**, 174–181 (2004)
- Minatti, E., Zanette, D.: Salt effects on the interaction of poly (ethylene oxide) and sodium dodecyl sulfate measured by conductivity. *Colloids Surf. A* **113**, 237–246 (1996)
- Soyama, H., Futakawa, M.: Estimation of cavitation intensity from the time taken for bubbles to develop. *Tribol. Lett.* **23**, 23–26 (2006)
- Chen, H.S., Li, Y.J., Chen, D.R., Wang, J.D.: Experimental and numerical investigations on development of cavitation erosion pits on solid surface. *Tribol. Lett.* **26**, 153–159 (2007)
- Prashad, H.: Diagnosis of rolling-element bearings failure by localized electrical current between track surfaces of races and rolling-elements. *J. Tribol.* **124**, 468–473 (2002)
- Chiou, Y.C., Lee, R.T., Lin, C.M.: Formation criterion and mechanism of electrical pitting on the lubricated surface under AC electric field. *Wear* **236**, 62–72 (1999)
- Jiang, H., Wong, P.L., Meng, Y., Wen, S.: An indirect electric field effect on the friction of boundary-lubricated contacts. *Lubri. Sci.* **15**, 275–292 (2003)
- Luo, J., Shen, M., Wen, S.: Tribological properties of nanoliquid film under an external electric field. *J. Appl. Phys.* **96**, 6733–6738 (2005)
- Lavielle, L.: Electric field effect on the friction of a polyethylene-terpolymer film on a steel substrate. *Wear* **176**, 89–93 (1994)
- Meng, Y., Hu, B., Chang, Q.: Control of local friction of metal/ceramic contacts in aqueous solutions with an electrochemical method. *Wear* **260**, 305–309 (2006)
- Krasucki, Z.: Breakdown of liquid dielectrics. *Proc. R. Soc. Lond. A* **294**, 393–403 (1966)
- Hu, Y., Granick, S.: Microscopic study of thin film lubrication and its contributions to macroscopic tribology. *Tribol. Lett.* **5**, 81–88 (1998)
- Luo, J., He, Y., Zhong, M., Jin, Z.: Gas micro-bubble phenomenon in nanoscale liquid film under external electric field. *Appl. Phys. Lett.* **89**, 0131041–0131043 (2006)

18. Luo, J., Wen, S.: Measuring technique and characteristics of thin film lubrication at nanoscale. In: Totten, G., Liang, H. (eds.) *Mechanical Tribology: Materials, Characterization, and Applications*, pp. 257–306. Marcel Dekker Inc., New York, (2004)
19. Luo, J., Wen, S., Huang, P.: Thin film lubrication, part I: the transition between EHL and thin film lubrication. *Wear* **194**, 107–115 (1996)
20. Lee, S., Müller, M., Ratoi-Salagean, M., Vörös, J., Pasche, S., De Paul, S.M., Spikes, H.A., Textor, M., Spencer, N.D.: Boundary lubrication of oxide surfaces by poly(L-lysine)-g-poly(ethylene glycol) (PLL-g-PEG) in aqueous media. *Tribol. Lett.* **15**, 231–239 (2003)
21. Tareev, B.: *Physics of dielectric materials*. Mir Publishers, Moscow (1975) [Translated from the Russian by Troitsky, A.]
22. Vorob'ev, V.S., Malyshenko, S.P., Petrin, A.B.: The role of an electrode in the formation of new phase nuclei in dielectrics. *J. Phys. D: Appl. Phys.* **35**, 257–266 (2002)
23. Gidon, S., Lemonnier, O., Rolland, B., Bichet, O., Dressler, C.: Electrical probe storage using Joule heating in phase change media. *Appl. Phys. Lett.* **85**, 6392–6394 (2004)
24. Mostowfi, F., Khristov, K., Czarnecki, J., Masliyah, J., Bhattacharjee, S.: Electric field mediated breakdown of thin liquid films separating microscopic emulsion droplets. *Appl. Phys. Lett.* **90**, 1847102 (2007)
25. Lewis, T.J.: Electronic processes in dielectric liquids under incipient breakdown stress. *IEEE Trans. Electr. Insul.* **20**, 123–132 (1985)